Published in final edited form as:
Sci Signal. ; 6(299): ra95. doi:10.1126/scisignal.2004225.

Convergence of G Protein-Coupled Receptor and Nitric Oxide Pathways Determines the Outcome to Cardiac Ischemic Injury

Z. Maggie Huang[1], **Erhe Gao**[1], **Fabio Fonseca**[2,3], **Hiroki Hayashi**[2,3], **Xiying Shang**[1], **Nicholas E. Hoffman**[1], **J. Kurt Chuprun**[1], **Xufan Tian**[4], **Doug G. Tilley**[1], **Muniswamy Madesh**[1], **David J. Lefer**[5], **Jonathan S. Stamler**[2,3,6], and **Walter J. Koch**[1,*]

[1]Center for Translational Medicine, Temple University School of Medicine, Philadelphia, PA, 19140, USA

[2]Institute for Transformative Molecular Medicine, Case Western Reserve University School of Medicine, Cleveland, Ohio, 44106, USA

[3]Department of Medicine, Case Western Reserve University, Cleveland, OH 44106, USA

[4]Department of Biochemistry, Thomas Jefferson University, Philadelphia, PA, 19107, USA

[5]Department of Surgery, Division of Cardiothoracic Surgery, Emory University School of Medicine, Atlanta, GA 30308, USA

[6]University Hospitals Harrington Discovery Institute, Cleveland, OH 44106, USA

Abstract

Heart failure caused by ischemic heart disease is a leading cause of death in the developed world. Treatment is currently centered on regimens involving G protein-coupled receptors (GPCRs) or nitric oxide (NO). These regimens are thought to target distinct molecular pathways. We showed that these pathways were interdependent and converged on the effector GRK2 (GPCR kinase 2) to regulate myocyte survival and function. Ischemic injury coupled to GPCR activation, including GPCR desensitization and myocyte loss, requires GRK2 activation, and we found that cardioprotection mediated by S-nitrosylation and inhibition of GRK2 depended on endothelial nitric oxide synthase (eNOS). Conversely, the cardioprotective effects of NO bioactivity were absent in a knock-in mouse with a form of GRK2 that cannot be S-nitrosylated. Because GRK2 and eNOS inhibit each other, the balance of the activities these enzymes in the myocardium determined the outcome to ischemic injury. Our findings suggest new insights into the mechanism of action of classic drugs used to treat heart failure and new therapeutic approaches to ischemic heart disease.

INTRODUCTION

Nitric oxide (NO) protects the heart against ischemic injury (1–3) and NO-based therapy is part of the standard of care in patients with heart failure (4). The classic view holds that NO acts primarily as a vasodilator; however, it is not known how NO protects the ischemic

*To whom correspondence should be addressed: walter.koch@temple.edu.

Author contributions: ZMH conducted all of the experiments and wrote the paper. EG and XS did ischemia/reperfusion, echocardiography and hemodynamics. HH and FF did the SNO-RAC experiments. JKC and XT performed cell studies. NEH did confocal imaging. DGT, MM and DJL contributed to the writing of the paper. JSS and WJK wrote the paper. WJK conceived and supervised the project.

Competing interests: The authors declare that they have no competing interests.

Materials availability: An MTA is required by Temple University for the GRK2-C340S knock-in mice.

heart. In this light, there has been growing appreciation that endogenous nitrosylating compounds called S-nitrosothiols are involved in ischemic cardioprotection (5, 6). The protein targets of S-nitrosothiols that may ameliorate cardiac injury are unknown.

GPCR kinase 2 (GRK2) is the primary effector of post-ischemic myocyte death that is downstream of GPCRs (7), particularly β-adrenergic receptors (βARs), which have a central role in the pathogenesis of heart failure (8). Although GPCR-based pathways of injury are viewed as unrelated to NO-based signaling, the inhibition of GRK2 by NO (9) would improve βAR resensitization and coupling to agonists, thus simulating the effect of β-blockade (10) (the lynchpin of the current treatment paradigm for heart failure). In fact, GRK2 appears to serve as critical regulator of myocardial GPCR signaling (11). Here we consider the possibility that classic GPCR-regulated ischemic injury and SNO-mediated cardioprotection have a shared mechanistic basis that arises through convergence of signaling on GRK2.

RESULTS

Cardiac eNOS protects against GRK2-mediated injury following ischemia

To determine whether classic cardioprotection by NO was mediated through inhibition of GRK2, we asked if eNOS could alleviate the detrimental effect of GRK2 activation following ischemia/reperfusion injury. For this purpose, we bred cardiac-specific GRK2 overexpressing transgenic (Tg) mice (12) with cardiac-specific eNOS Tg mice (1) to generate GRK2 and eNOS double transgenic mice (GRK2/eNOS mice). GRK2 and eNOS abundance in the hearts of GRK2/eNOS mice were similar to those in the breeder lines (fig. S1A). We then subjected adult GRK2/eNOS mice and their littermates (including control mice and single-breeder Tg mice) to 30 min of myocardial ischemia followed by 24 hours of reperfusion (13). Consistent with a previous report (7), GRK2 Tg mice had larger infarcts at 24 hours compared to the other lines (Fig. 1, A and B), whereas eNOS Tg mice had reduced infarcts. Infarct size in GRK2/eNOS mice was reduced by 20% compared to GRK2 Tg mice and was not different from control mice (Fig. 1, A and B). All four groups had similar ischemic areas at risk (fig. S1B), demonstrating the same severity of ischemic stress.

Infarct size reductions in GRK2/eNOS mice translated to marked improvements (~30%) in cardiac function as measured by left ventricular (LV) ejection fraction (EF%) by echocardiography 24 hours post-reperfusion (Fig. 1C, fig. S1C). In addition, LV dilatation in GRK2 Tg mice (as assessed by diastolic LV internal diameter) was accounted for, and inversely correlated with, myocardial eNOS expression (fig. S1D). To further explore the functional relationship between eNOS and GRK2 in the ischemic heart, we bred GRK2 Tg mice with $eNOS^{null}$ mice and subjected these mice to ischemia/reperfusion injury. Deletion of eNOS exacerbated the post-ischemia/reperfusion injury caused by GRK2 as demonstrated by larger infarct size in GRK2/$eNOS^{null}$ mice compared to the GRK2 Tg mice or $eNOS^{null}$ alone (Fig. 1D) despite similar ischemic areas at risk (fig. S1E). Thus, the injurious effects of GRK2 in the ischemic heart is accentuated by deficiency of eNOS and attenuated by increased eNOS.

Inhibition of GRK2 by the peptide inhibitor βARKct protects against cardiac ischemic injury (7), and βARKct Tg mice showed robust protection against ischemia/reperfusion injury as measured by infarct size at 24 hours (Fig. 1E, fig. S1F). When βARKct mice were bred onto the $eNOS^{null}$ background, cardioprotection was abolished and infarct size was no different in βARKct/$eNOS^{null}$ mice than in control mice (Fig. 1E, fig. S1F). These data argue that the protection conferred by GRK2 inhibition is transduced through eNOS. Our findings are consistent with a model in which GRK2 inhibits eNOS activity and inhibition of GRK2 allows for increased NO bioavailability.

GRK2 interacts with eNOS in mouse heart

We next explored the mechanism of this apparent interdependence of eNOS and GRK2 activity. eNOS co-immunoprecipitated with GRK2 from cardiac lysates (Fig. 2A) and this interaction was increased substantially after 30 min of ischemia followed by 30 min of reperfusion (Fig. 2, B and C). We overexpressed eNOS in neonatal rat ventricular myocytes (NRVMs) with or without GRK2 co-expression and treated myocytes with H_2O_2 to simulate oxidative stress in ischemia/reperfusion injury. H_2O_2 treatment activated eNOS (as measured by phosphorylation of Ser^{1177}) and eNOS activation was blocked by GRK2 co-expression (Fig. 2, D and E). These findings are consistent with reports that GRK2 Tg hearts have lower NO concentrations following ischemia (7) and that GRK2 directly binds Akt (14), leading to lower Akt-mediated phosphorylation of eNOS and thus activity. Akt may be part of a protein complex with GRK2-eNOS.

We assessed the S-nitrosylation state of GRK2 after ischemia/reperfusion injury. Because S-nitrosylation inhibits GRK2 (9), the amount of nitrosylated GRK2 should reflect the extent to which GRK2 was inhibited by eNOS and thus the tendency for injury (lower amounts of nitrosylated GRK2) compared to protection (higher amounts of nitrosylated GRK2). Amounts of SNO-GRK2 were determined with a Cys-NO specific antibody (15) following immunoprecipitation of GRK2 from hearts of GRK2 Tg mice and GRK2/eNOS mice. The SNO-GRK2/GRK2 ratio in post-ischemia/reperfusion samples was decreased by 28% in GRK2 Tg mice compared to sham operated controls, whereas co-expression of eNOS (in GRK2/eNOS mice) normalized the amount of cardiac SNO-GRK2, which was comparable to sham controls (Fig. 2, F and G). Thus, overexpression of eNOS overcomes GRK2-mediated inhibition of eNOS to block GRK2 activity, and ultimately portends better outcomes after ischemic injury. Overall, these data demonstrate bi-directional and dynamic regulation of eNOS and GRK2 activities and suggest that the heart's response to ischemic insult lies in the balance.

GRK2-C340S knock-in mice are resistant to S-nitrosylation-based regulation

To examine the importance of GRK2 in the cardioprotection conferred by eNOS, we generated a knock-in mouse harboring a point mutation in GRK2 ($Cys^{340}\rightarrow$Ser; C340S) that prevented the majority of S-nitrosylation by which NO inhibits GRK (9) (fig S2, A and B). The abundance of GRK2 in multiple organs including the heart was similar to that in wild-type control mice (Fig. 3A). There were also no compensatory changes in the abundance of mRNAs encoding β_1AR, β_2AR, GRK3, GRK5, GRK6 or adenylyl cyclase (AC) 5 and AC6 in the hearts of GRK2-C340S knock-in mice compared to wild-type mice (fig. S2). The abundance of major limiting factors in βAR signaling, including AC5, AC6, and Gαs, were also not altered (fig. S2) and we observed no cardiac functional differences in C340S mice compared to wild-type mice (fig. S3).

GRK2-C340S knock-in mice were resistant to S-nitrosylation-based regulation. The SNO-RAC assay (16) showed that the amounts of S-nitrosylated GRK2 increased in the hearts of wild-type mice following isoproterenol infusion but not in GRK2-C340S knock-in hearts (Fig. 3, B and C). Similarly, S-nitrosoglutathione (GSNO) infusion (for 7 days) increased S-nitrosylation of GRK2 in the hearts of wild-type mice but not in GRK2-C340S hearts (fig. S4, A and B). These data that establish Cys^{340} in GRK2 is modified by both endogenous and exogenous NO or nitrosothiol (SNO). S-nitrosylation of Cys^{340} did not appear to affect the interaction between GRK2 and eNOS because the association between these two proteins was similar in wild-type and GRK2-C340S knock-in hearts (fig. S4, C and D). The GRK2-eNOS interaction in the GRK2-C340S knock-in hearts was increased post ischemia/reperfusion, similar to that in wild-type hearts (fig. S4, E and F). Global amounts of S-nitrosothiols in the heart were not changed by the C340S mutation under basal conditions

(fig. S4, G and H). S-nitrosylated GRK2 was, however, decreased in the GRK2-C340S knock-in hearts compared to wild-type hearts post ischemia/reperfusion (fig. S4 I).

Ischemic heart failure is characterized by both myocyte injury and βAR desensitization. If the cardioprotective effects of NO are mediated through GRK2 S-nitrosylation, GRK2-C340S mice should be resistant to NO. We first employed an in vivo assay for βAR desensitization (9), which analyzes the waning of cardiac pressure over time during a maintained infusion of isoproterenol. GRK2-C340S mice exhibited greater loss of contractility than wild-type animals (Fig. 3D). Thus, desensitization during maintained catecholamine stimulation was accelerated in GRK2-C340S mice, a finding that is consistent with higher GRK2 activity. Moreover, the NOS inhibitor L-NG-nitroarginine methyl ester (L-NAME), which promoted βAR desensitization in wild-type animals (fig. S5A), had minimal effect in GRK2-C340S mice (fig. S5B). These data establish that agonist stimulation of the βAR is coupled to eNOS-mediated S-nitrosylation of GRK2, which prevents cardiac receptor desensitization. Diminished NO bioactivity causes overt βAR uncoupling from agonist stimulation, a major problem in the failing heart.

GRK2-C340S knock-in mice are more susceptible to ischemia/reperfusion injury

The interdependence of GRK2 and eNOS was further explored using GRK2 C340S mice. GRK2-C340S mice had larger infarcts following ischemia/reperfusion than wild-type mice despite having similar areas at risk (Fig. 4, A and B, fig. S6A). These results suggest that GRK2 C340S mutant mice had higher GRK2 activity. Furthermore, the NOS inhibitor L-NAME increased ischemic injury in wild-type but not in mutant mice (Fig. 4B). Moreover, infusion of GSNO reduced infarct size in both wild-type mice and GRK2 overexpressing mice, but not in GRK2-C340S mice (Fig. 4, C and D, fig. S6, B and C). Functional assessments of cardiac performance correlated well with infarct size: GRK2-C340S mice had significantly worse post-ischemia/reperfusion cardiac function than wild-type mice; L-NAME treatment worsened cardiac function in wild-type mice but not in GRK2-C340S mice (fig. S6D); GSNO infusion improved post-ischemia/reperfusion cardiac function in wild-type mice and GRK2 Tg mice but not in GRK2-C340S mice (fig. S6, E and F). Similarly, mice that overexpressed eNOS and had GRK2-C340S were not protected after ischemia/reperfusion injury (fig. S7, A and B). Therefore, the cardioprotective effects of both endogenous and exogenous NO are mediated by S-nitrosylation of GRK2. Our data should not be taken to indicate that GRK2 inhibition is the only means by which NO bioactivity may protect the heart (by analogy to the multiple mechanisms by which NO may inhibit apoptosis) and it should be noted that the protective effects of SNOs may vary in different ischemia/reperfusion models (fig. S7, C and D) (17).

To test whether the different outcome to ischemia/reperfusion injury in C340S knock-in mice is accompanied by altered survival signaling, we measured amounts of phosphorylated and activated Akt in the injured hearts (Fig. 4E). Ischemia/reperfusion resulted in robust activation Akt in both groups, but to a lesser extent in GRK2-C340S knock in mice, consistent with the worsened phenotype in these mice (Fig. 4F). Also, after ischemia/reperfusion injury, the border zone of C340S hearts showed more apoptotic nuclei in ischemic myocytes than in wild-type hearts (Fig. 4, G, I, and H). GSNO infusion reduced cell death after ischemia/reperfusion injury wild-type hearts but not in C340S hearts (Fig. 4, G and I). We also found no difference in EGFR activity in cardiomyocytes overexpressing wild-type GRK2 or GRK2-C340S following stimulation of βARs with isoproterenol (fig. S8, A and B), eliminating the possibility that trans-activation of the epidermal growth factor receptor (EGFR) by GRK5/6 was involved in cardioprotection (18). Myocyte injury by GRK2 is thus likely mediated through direct pro-death kinase activity. Taken together, these data provide strong evidence for (i) pro-death effects of GRK2 that involve loss of NO bioactivity and (ii) protective functions of eNOS that involve inhibition of GRK2.

DISCUSSION

Our results demonstrate that GRK2 and eNOS interact in the heart to form a key nodal point that determines outcomes to ischemic injury. GRK2-eNOS disequilibrium (increased GRK2 activity or decreased eNOS activity) manifests as βAR desensitization and myoctye injury, which are molecular corollaries of heart failure. eNOS inactivates GRK2 by S-nitrosylation to enable signaling through βARs, thereby maintaining cardiac function. Ischemic stress and heart failure are typified by increased abundance of GRK2 (11, 19), which counteracts eNOS cardioprotection (Fig. 4J). The utility of nitrates (a source of NO bioactivity) and β-blockers (a means to inhibit GRK2 activity) (20, 21) in heart failure has preceded detailed molecular understanding. Our data indicate that these drugs may restore the balance between GRK2 and NO activity and suggest new therapeutic approaches.

GRK2 has been previously reported to directly bind to Akt (14), leading to lower Akt-mediated eNOS phosphorylation and activity. The finding that cardioprotection mediated by GRK2 inhibition is dependent on eNOS (because no cardioprotection is seen in βARKct/eNOS^{null} mice) is consistent with involvement of Akt. Our data (Fig. 4J) thus raise the possibility that Akt may be part of a signaling complex with GRK2-eNOS. It is interesting to note that activation of the Akt/eNOS pathway is dependent on $G_{\beta\gamma}$ and βARKct inhibits GRK2 by blocking $G_{\beta\gamma}$.

Current tenets hold that cardioprotection by NO is mediated by various effects on vessel tone, thrombosis, cell death signaling, inflammation and energy conservation, and a long list of nitrosylated targets (guanylate cyclase, caspases, NF-κB, and mitochondrial proteins) have been investigated (23). More than one thousand S-nitrosylated proteins have been identified in hearts treated with NO donors, and consequently, it is intriguing that a single cysteine in GRK2 (Cys^{340}) is the primary locus through which both endogenous and exogenous NO bioactivity confer protection (Fig. 4J). Inhibition of GRK2 by NO can thus account for a major part of NO's protective function in the ischemic heart. It is interesting to note in this regard that GRK2 translocates to mitochondria following ischemia/reperfusion (24) and that mitochondrially-targeted NO bioactivity is protective in ischemia/reperfusion models (17, 25). Mitochondrial targets of GRK2 could be effectors of death kinase activity.

Our results suggest that GRK2 is a common factor underlying the cardioprotective effects of NO and β blockers as well as newer therapeutic strategies, which all yield beneficial effects in heart failure models (26–28). Thus our new results support the idea that GRK2 is a potential therapeutic target in acute ischemia and identify a deficiency of NO bioactivity as a component of the pathophysiology of death kinase signaling. Our studies have implications for GPCR signaling in the ischemic heart, broaden perspectives on βAR blocker therapy, and point to new therapeutic approaches in acute coronary syndromes, chronic myocardial ischemia and heart failure.

MATERIALS AND METHODS

Generation of GRK2-C340S knock-in mice

A GRK2 positive clone was screened from a 129/SV mouse genome BAC (bacterial artificial chromosome) library (obtained from Children's Hospital Oakland Research Institute) and the G was replaced with C in codon 340 leading to Cys$^{340}\rightarrow$Ser (C340S) mutation in exon 12. The GRK2 C340S targeting vector consisted of the diphtheria toxin A (DTA) gene, a 3.5Kb 5′ homology sequence, the neomycin resistance gene (Neo) and a 3.4 Kb 3′ homology sequence which contained the mutation. The linearized targeting vector was electroporated into C57 embryonic stem cells. Positive clones were injected to generate

chimeric mice and GRK2-C340S mice (Ingenious Targeting Laboratory, Stony Brook, NY). Mutation was confirmed by sequencing of PCR products flanking exon 12.

Ischemia/Reperfusion Injury Model

Surgical procedures were carried out according to National Institutes of Health Guidelines on the Use of Laboratory Animals and all procedures were approved by the Animal Care Committee at Temple University. The ischemia/reperfusion injury protocol was performed as previously described with minor modifications (13). Briefly, 8–10 week old mice were anesthetized with 3% isoflurane inhalation. The heart was exposed through a left thoracotomy at the level of the fifth intercostal space. A slipknot was made around the left anterior descending coronary artery (LAD) at the level of the left auricle with a 6-0 silk suture. After the slipknot was tied, the heart was immediately placed back into the intrathoracic space followed by evacuation of pneumothoraces and closure of the muscle and skin suture through a previously placed purse-string suture. Sham-operated animals were subjected to the same surgical procedures except that the suture was passed under the LAD but was not tied. Following 30 min of ischemia, the slipknot was released and the myocardium was reperfused for either 3 hours to determine myocardial apoptosis, or 24 hours to assess myocardial infarct size and cardiac function. For some of the mice GSNO (10mg/kg/day) or PBS was infused via implanted micro-osmotic pumps (Alzet, Cupertino, CA) for 24 hours or 7 days prior to ischemia/reperfusion surgery, and in other experiments L-NAME (50nmol/g, bolus) was injected 10 min prior to ischemia/reperfusion surgery.

Determination of LV Infarct Size and Area at Risk

LV infarct size and area at risk was determined as previously described with slight modifications (13). Briefly, the ligature around the LAD was re-tied through the previous ligation and 0.2 ml 2% Evans blue dye was injected 24 hours post reperfusion. The dye distributed uniformly in the heart to areas perfused by the non-ligated coronary arteries. The heart was then excised and sliced into five 1.2 mm-thick sections in the short axis of the heart. The sections were then stained in 2% triphenyltetrazolium chloride (TTC) (Sigma-Aldrich, St. Louis, MO) in PBS at room temperature for 15 min and then digitally photographed. TTC-negative staining region will be pale and TTC-positive staining region will be red. The areas were defined as follows: the infarct area (Inf) consists of the TTC-negative staining region, the area at risk (AAR) consists of the Evan's Blue negatively staining region – including the TTC-positive staining and TTC-negative staining regions, and the area not at risk (ANAR) or non-ischemic region consists of the Evan's blue positively staining regions. These regions were quantified using SigmaScan Pro 5.0 (SPSS Science, Chicago, IL). Myocardial infarct size was calculated as a percentage of the AAR (Inf/AAR) and the AAR was calculated as the percentage of total LV (AAR/(AAR +ANAR)).

Transthoracic Echocardiographic Analysis

Transthoracic two-dimensional echocardiography in mice anesthetized with 2% isoflurane was performed with a 12-MHz probe as described previously (13). M-mode echocardiography was carried out in the parasternal short axis in mice 24 hours post reperfusion to assess heart rate (HR), left ventricular (LV) end-diastolic diameter (LVEDD), LV anterior and posterior wall thickness (LVAWT and LVPWT, respectively). LV fractional shortening (FS%) and ejection fraction (EF%) were calculated.

Hemodynamic Analysis of Cardiac Function

Hemodynamic analysis was conducted as described previously (9). Briefly, a 1.4 French micromanometer-tipped catheter (Millar instruments, Houston, TX) was inserted into the

right carotid artery and then advanced into the LV. A polyethylene-50 catheter was placed in the left external jugular vein for continuous infusion of Iso (20 ng/g/min) for 30 min. WT or GRK2-C340S knock-in mice were pre-treated with either PBS or L-NAME (50 nmol/g, bolus) for 10 min. Steady state LV maximal ($dp/dt_{max.}$) was recorded in closed-chest mode throughout the experiment using a Powerlab DAQ System (Millar Instrument).

Assessment of Myocardial Apoptosis

Myocardial apoptosis was assessed by terminal deoxynucleotidyl-transferase mediated dUTP nick end labeling (TUNEL) staining (7). Mice (n=4–6 for sham groups, n=6–8 for I/R groups) were euthanized 3 hours post reperfusion, and hearts were quickly removed and fixed in 4% paraformaldehyde. The hearts were then embedded in paraffin and cut into sections measuring 6 μm in thickness. TUNEL staining of sections was carried out using the *in situ* cell death detection kit (Roche, Indianapolis, IN). Slides were counterstained with DAPI-containing mounting media. Cardiac myocytes were labeled with Troponin I Ab (Cell Signaling Technologies, Beverly, MA). The infarct border zone was visualized under a fluorescence microscope with the DAPI filter (330–380 nm) and a FITC filter (465–495 nm), and digital images were collected for DAPI, FITC, and merged. Images for >3 sections per animal were taken. Apoptotic cells with green fluorescence were counted using NIS Elements Software (Nikon, Japan) to assess the apoptotic index (number of TUNEL positive nuclei/number of total nuclei). More than 1000 cells were counted for each heart. For some experiments, sections were imaged using a Carl Zeiss 710 two-photon confocal microscope with a W Plan-Apochromat 63x oil objective, using 1x digital zoom, with excitations at 405, 488, and 561nm. Images were quantified using Zen 2010 (Zeiss).

Isolation and primary culture of neonatal rat ventricular cardiomyocytes

Ventricular cardiomyocytes from 1–2-day-old rat hearts (neonatal rat ventricular myocytes; NRVMs) were prepared as described before (7). NRVMs were cultured in Ham's F-10 supplemented with 5% fetal bovine serum (FBS), penicillin/streptomycin (100 units/ml) at 37°C in a 95% air/5% CO_2 humidified atmosphere for 4 days. NRVMs were infected with the indicated adenoviruses at a multiplicity of infection of 20 on day 2, and experiments were performed 48 hours post infection. NRVMs were starved in 0.5% FBS 8 hours before H_2O_2 treatment (150 μM, 10 min).

Co-Immunoprecipitation and Immunoblotting

Cells and tissue were homogenized in ice-cold RIPA buffer (50mMol/L Tris-HCl, 135mMol/L NaCl, 1% NP-40, 0.5% Sodium Deoxycholate, 0.1% SDS, supplemented with 1mMol/L PMSF, 10μg/ml Leupeptin, 20μg/ml Aprotinin, and 1% (v/v) phosphatase inhibitor cocktail 1 and 2 (Sigma-Aldrich, St. Louis, MO). The lysates were centrifuged at 13,000 rpm for 30 minutes at 4°C and protein concentration was determined using BCA Protein Assay (Pierce, Rockford, IL). Equal amounts of protein were then heated at 95°C for 5 minutes in 6X protein loading buffer. For co-immunoprecipitation (co-IP), endogenous GRK2 from equal amounts of heart lysates was immunoprecipitated (IP) with rabbit GRK2 Ab conjugated to protein A/G agarose beads (Santa Cruz, Biotechnology, Santa Cruz, CA). Samples were rotated overnight at 4°C and then centrifuged at 5,000 rpm for 5 min. IP'd samples were washed three times with lysis buffer and resuspended in 1x gel loading buffer and boiled. Clarified lysates and immunocomplexes were electrophoresed through 4–20% polyacrylamide gels and transferred to nitrocellulose membranes. Membranes were blocked in Odyssey Blocking Buffer (Li-COR, Lincoln, NE), and then incubated with primary antibodies detecting total p42/44 extracellular signal-regulated kinase (ERK1/2), p42/44 ERK, total Akt, pAkt, total eNOS, peNOS (Cell Signaling Technologies), GRK2, AC 5/6, Gαs (Santa Cruz Biotechnology, Santa Cruz, CA), GAPDH (Millipore, Billerica, MA), and

S-nitroso-Cysteine (Sigma-Aldrich, St. Louis, MO) at 4°C overnight. Proteins were then detected using the appropriate Alexa Fluor 680nm- or IRDye 800nm-coupled secondary antibodies (Life Technologies, Carlsbad, California) using the Odyssey Infrared Imaging System (Li-COR, Lincoln, NE). Quantitative densitometric analysis was performed using Odyssey infrared imaging software (version 2.1). Phospho-specific antibodies signals and S-nitrosylation signals were normalized to total antibody signal.

SNO-RAC assay and global S-nitrosothiols measurement

Protein S-nitrosylation was detected by SNO-RAC (resin assisted capture) as previously described (16). Briefly, hearts were homogenized by polytron homogenizer and centrifuged. Supernatant were collected and diluted in HEN buffer (100 mM HEPES, 1 mM EDTA, 0.1 mM neocuproine, pH7.7) with 1% SDS and the 0.1 % methyl methanethiosuflonate (MMTS) for blocking thiol for 20 min at 50 °C. Samples were then precipitated with acetone and washed with 70% acetone twice. Following the addition of 50 μl thiopropyl sepharose and 50 mM sodium ascorbate, samples were rotated in the dark for 4 h. Eluted samples after wash were analyzed by Western blot. Global S-nitrosothiol amounts were measured using photolysis chemiluminescence (29).

Real-Time PCR

Total RNA from the hearts of 8 weeks old WT and GRK2 C340S hearts were extracted using TRIzol (Life Technologies) and reverse transcribed with random primers (Biorad, Hercules, CA). The primers used for quantitative RT-PCR included: 1). β1-AR: forward: 5′-GTCATGGGATTGCTGGTGGT-3′, reverse: 5′-GCAAACTCTGGTAGCGAAAGG-3′; 2). β2-AR: forward: 5′-GGGAACGACAGCGACTTCTT-3′, reverse: 5′-GCCAGGACGATAACCGACAT-3′; 3). GRK3: forward: 5′-GTGTGTGCGCGATACATTGC-3′, reverse: 5′-GGGCTACATACCCCAGAGATAC-3′; 4). GRK5: forward: 5′-CCTCCGAAGGACCATAGACA-3′, reverse: 5′-GACTGGGGACTTTGGAGTGA-3′; 5). GRK6: forward: 5′-TGACCCACGAGTACCTGAG-3′, reverse: 5′-TCGCTTCTTTATCCGCTTCTTTT-3′; 5). AC5: forward: 5′-CTTGGGGAGAAGCCGATTCC-3′, reverse: 5′-ACCGCTTAGTGGAGGGTCT-3′; 6). AC6: forward: 5′-GATGAACGGAAAACAGCTTGGG-3′, reverse: 5′-GGTGGCTCCGCATTCTTGA-3′; 7). GAPDH: forward: 5′-CCACTCTTCCACCTTCGATG-3′, reverse: 5′-TCCACCACCCTGTTGCTGTA-3′. Real-Time quantification was performed by cyber green (Biorad) using Biorad CFR96 detection system (Biorad). Relative gene expression was normalized to that of GAPDH and compared using Δ(ΔCt) method between wild-type and GRK2-C340S counterpart.

Supplementary Material

Refer to Web version on PubMed Central for supplementary material.

Acknowledgments

We thank Drs. Ju Chen, Hongqiang Chen, Gregory Pari and Yang Gao for assistance with BAC recombineering, Dr. Joseph Rabinowitz for adenoviruses, and Zuping Qu, Jessica Ibetti, Samantha Baxter and Nicholas Otis for technical support.

Funding: This work was supported in part by National Institutes of Health grant R37 HL061690 (WJK), P01 HL08806 (Project 3, WJK), P01 HL075443 (Project 2, WJK) and P01 HL075443 (Project 3, JSS), also a post-doctoral fellowship grant from the Great Rivers Affiliate of the American Heart Association (ZMH).

References and Notes

1. Elrod JW, Greer JJ, Bryan NS, Langston W, Szot JF, Gebregzlabher H, Janssens S, Feelisch M, Lefer DJ. Cardiomyocyte-specific overexpression of NO synthase-3 protects against myocardial ischemia-reperfusion injury. Arterioscler Thromb Vasc Biol. 2006; 26:1517–1523. [PubMed: 16645153]
2. Nakanishi K, Vinten-Johansen J, Lefer DJ, Zhao Z, Fowler WC, McGee DS, Johnston WE. Intracoronary L-arginine during reperfusion improves endothelial function and reduces infarct size. Am J Physiol. 1992; 263:H1650–H1658. [PubMed: 1336313]
3. Weyrich AS, Ma XL, Lefer AM. The role of L-arginine in ameliorating reperfusion injury after myocardial ischemia in the cat. Circulation. 1992; 86:279–288. [PubMed: 1319855]
4. Taylor AL, Ziesche S, Yancy C, Carson P, D'Agostino R, Ferdinand K, Taylor M, Adams K, Sabolinski M, Worcel M, Cohn JN. Combination of isosorbide dinitrate and hydralazine in blacks with heart failure. N Engl J Med. 2004; 351:2049–2057. [PubMed: 15533851]
5. Kohr MJ, Sun J, Aponte A, Wang G, Gucek M, Murphy E, Steenbergen C. Simultaneous measurement of protein oxidation and S-nitrosylation during preconditioning and ischemia/reperfusion injury with resin-assisted capture. Circ Res. 2011; 108:418–426. [PubMed: 21193739]
6. Lima B, Lam GK, Xie L, Diesen DL, Villamizar N, Nienaber J, Messina E, Bowles D, Kontos CD, Hare JM, Stamler JS, Rockman HA. Endogenous S-nitrosothiols protect against myocardial injury. Proc Natl Acad Sci U S A. 2009; 106:6297–6302. [PubMed: 19325130]
7. Brinks H, Boucher M, Gao E, Chuprun JK, Pesant S, Raake PW, Huang ZM, Wang X, Qiu G, Gumpert A, Harris DM, Eckhart AD, Most P, Koch WJ. Level of G protein-coupled receptor kinase-2 determines myocardial ischemia/reperfusion injury via pro- and anti-apoptotic mechanisms. Circ Res. 2010; 107:1140–1149. [PubMed: 20814022]
8. Bristow MR, Ginsburg R, Minobe W, Cubicciotti RS, Sageman WS, Lurie K, Billingham ME, Harrison DC, Stinson EB. Decreased catecholamine sensitivity and beta-adrenergic-receptor density in failing human hearts. N Engl J Med. 1982; 307:205–211. [PubMed: 6283349]
9. Whalen EJ, Foster MW, Matsumoto A, Ozawa K, Violin JD, Que LG, Nelson CD, Benhar M, Keys JR, Rockman HA, Koch WJ, Daaka Y, Lefkowitz RJ, Stamler JS. Regulation of beta-adrenergic receptor signaling by S-nitrosylation of G-protein-coupled receptor kinase 2. Cell. 2007; 129:511–522. [PubMed: 17482545]
10. Gilbert EM, Abraham WT, Olsen S, Hattler B, White M, Mealy P, Larrabee P, Bristow MR. Comparative hemodynamic, left ventricular functional, and antiadrenergic effects of chronic treatment with metoprolol versus carvedilol in the failing heart. Circulation. 1996; 94:2817–2825. [PubMed: 8941107]
11. Huang ZM, Gold JI, Koch WJ. G protein-coupled receptor kinases in normal and failing myocardium. Front Biosci. 2011; 16:3047–3060.
12. Koch WJ, Rockman HA, Samama P, Hamilton RA, Bond RA, Milano CA, Lefkowitz RJ. Cardiac function in mice overexpressing the beta-adrenergic receptor kinase or a beta ARK inhibitor. Science. 1995; 268:1350–1353. [PubMed: 7761854]
13. Gao E, Lei YH, Shang X, Huang ZM, Zuo L, Boucher M, Fan Q, Chuprun JK, Ma XL, Koch WJ. A novel and efficient model of coronary artery ligation and myocardial infarction in the mouse. Circ Res. 2010; 107:1445–1453. [PubMed: 20966393]
14. Liu S, Premont RT, Kontos CD, Zhu S, Rockey DC. A crucial role for GRK2 in regulation of endothelial cell nitric oxide synthase function in portal hypertension. Nat Med. 2005; 11:952–958. [PubMed: 16142243]
15. Shan J, Betzenhauser MJ, Kushnir A, Reiken S, Meli AC, Wronska A, Dura M, Chen BX, Marks AR. Role of chronic ryanodine receptor phosphorylation in heart failure and β-adrenergic receptor blockade in mice. J Clin Invest. 2010; 120:4375–4387. [PubMed: 21099115]
16. Forrester MT, Thompson JW, Foster MW, Noguira L, Moseley MA, Stamler JS. Proteomic analysis of S-nitrosylation and denitrosylation by resin-assisted capture. Nat Biotechnol. 2009; 27:557–559. [PubMed: 19483679]
17. Anand P, Hess DT, Stamler JS. Identifying SNO sites with Cardioprotection. Circ Res. in press.

18. Noma T, Lemaire A, Naga Prasad SV, Barki-Harrington L, Tilley DG, Chen J, Le Corvoisier P, Violin JD, Lefkowitz RJ, Rockman HA. Beta-arrestin-mediated beta1-adrenergic receptor transactivation of the EGFR confers cardioprotection. J Clin Invest. 2007; 117:2445–2458. [PubMed: 17786238]
19. Rockman HA, Koch WJ, Lefkowitz RJ. Seven-transmembrane-spanning receptors and heart function. Nature. 2002; 415:206–212. [PubMed: 11805844]
20. Iaccarino G, Tomhave ED, Lefkowitz RJ, Koch WJ. Reciprocal in vivo regulation of myocardial G protein-coupled receptor kinase expression by beta-adrenergic receptor stimulation and blockade. Circulation. 1998; 98:1783–1789. [PubMed: 9788834]
21. Rengo G, Lymperopoulos A, Zincarelli C, Donniazuo M, Soltys S, Rabinowitz JE, Koch WJ. Myocardial adeno-associated virus serotype 6-betaARKct gene therapy improves cardiac function and normalizes the neurohormonal axis in chronic heart failure. Circulation. 2009; 119:89–98. [PubMed: 19103992]
22. Taguchi K, Kobayashi T, Takenouchi Y, Matsumoto T, Kamata K. Angiotensin II causes endothelial dysfunction via the GRK2/Akt/eNOS pathway in aortas from a murine type 2 diabetic model. Pharmacol Res. 2011; 64:535–546. [PubMed: 21571071]
23. Haldar SM, Stamler JS. S-nitrosylation: integrator of cardiovascular performance and oxygen delivery. J Clin Invest. 2013; 123:101–110. [PubMed: 23281416]
24. Chen M, Sato PY, Chuprun JK, Peroutka RJ, Otis NJ, Ibetti J, Pan S, Sheu SS, Gao E, Koch WJ. Prodeath signaling of G protein-coupled receptor kinase 2 in cardiac myocytes after ischemic stress occurs via extracellular signal-regulated kinase-dependent heat shock protein 90-mediated mitochondrial targeting. Circ Res. 2013; 112:1121–1134. [PubMed: 23467820]
25. Prime TA, Blaikie FH, Evans C, Nadtochiy SM, James AM, Dahm CC, Vitturi DA, Patel RP, Hiley CR, Abakumova I, Requejo R, Chouchani ET, Hurd TR, Garvey JF, Taylor CT, Brookes PS, Smith RA, Murphy MP. A mitochondria-targeted S-nitrosothiol modulates respiration, nitrosates thiols, and protects against ischemia-reperfusion injury. Proc Natl Acad Sci U S A. 2009; 106:10764–10769. [PubMed: 19528654]
26. Ungerer M, Böhm M, Elce JS, Erdmann E, Lohse MJ. Altered expression of beta-adrenergic receptor kinase and beta 1-adrenergic receptors in the failing human heart. Circulation. 1993; 87:454–463. [PubMed: 8381058]
27. White DC, Hata JA, Shah AS, Glower DD, Lefkowitz RJ, Koch WJ. Preservation of myocardial beta-adrenergic receptor signaling delays the development of heart failure after myocardial infarction. Proc Natl Acad Sci U S A. 2000; 97:5428–5433. [PubMed: 10779554]
28. Maurice JP, Shah AS, Kypson AP, Hata JA, White DC, Glower DD, Koch WJ. Molecular beta-adrenergic signaling abnormalities in failing rabbit hearts after infarction. Am J Physiol. 1999; 276:H1853–H1860. [PubMed: 10362663]
29. Hausladen A, Rafikov R, Angelo M, Singel DJ, Nudler E, Stamler JS. Assessment of nitric oxide signals by triiodide chemiluminescence. Proc Natl Acad Sci U S A. 2007; 104:2157–2162. [PubMed: 17287342]

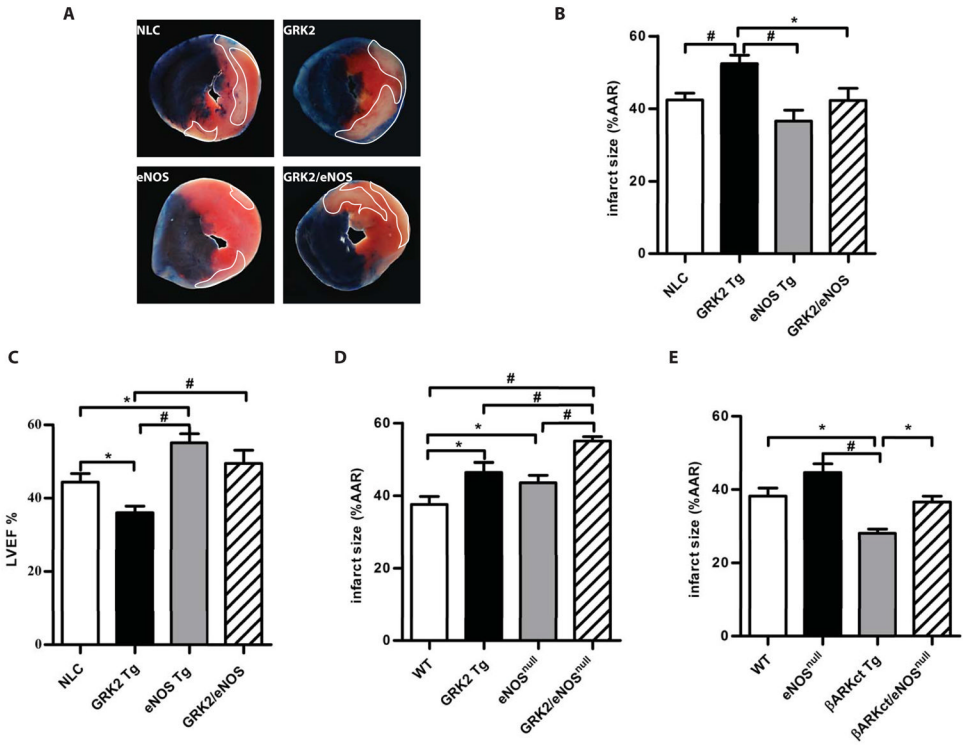

Fig. 1.

Cardiac eNOS protects against GRK2-mediated injury following ischemia/reperfusion. **A**, Representative images of Evan's Blue/triphenyltetrazolium chloride (TTC) staining of hearts after ischemia/reperfusion. Dotted area is the infarct zone. **B**, Quantification of infarct size as a percentage of left ventricular (LV) ischemic area at risk (AAR) in non-transgenic control (NLC), GRK2 Tg, eNOS Tg and GRK2/eNOS mice. *, $P<0.05$, #, $P<0.01$ (ANOVA, n = 8–12 mice/group). **C**, Cardiac function evaluated by LV ejection fraction (EF %) measured by echocardiography in the mice from (**B**). *, $P<0.05$, #, $P<0.01$ (ANOVA, n = 8–12 mice/group). **D**, Quantification of infarct size as a percentage of LV AAR in wild-type control (WT), GRK2 Tg, $eNOS^{null}$ and $GRK2/eNOS^{null}$ mice. *, $P<0.05$, #, $P<0.01$ (ANOVA, n = 10–12 mice/group). **E**, Quantification of infarct size as a percentage of LV AAR in WT, βARKct Tg, $eNOS^{null}$ and $\beta ARKct/eNOS^{null}$ mice. *, $P<0.05$, #, $P<0.001$ (ANOVA, n = 6–8 mice/group).

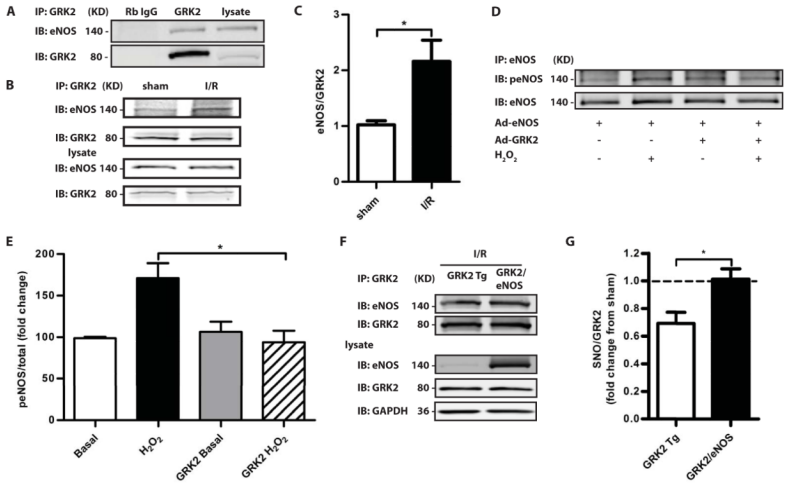

Fig. 2.

GRK2 interacts with eNOS in mouse heart, an interaction that is increased after ischemia. **A, B**, Representative Western blots of GRK2 and eNOS co-immunoprecipitations at baseline (**A**), and post-ischemia-reperfusion (**B**). **C**, Quantification of the amount of cardiac eNOS immunoprecipitated by GRK2 in sham treated mice and mice after ischemia-reperfusion with eNOS/GRK2 (mean±SEM) values shown. *, $P<0.05$ (Mann-Whitney test, n=5 mice/group). **D**, Activation of eNOS induced by H_2O_2 treatment is blocked by co-expression of GRK2 in myocytes. eNOS was immunoprecipitated from NRVMs infected with an adenovirus containing eNOS (Ad-eNOS), with or without Ad-GRK2, and treated with H_2O_2. A representative Western blot for eNOS phosphorylated at Ser^{1177} (top panel) and total eNOS (bottom panel) is shown. **E**, Quantification of 5 separate experiments done as in (**D**). *, $P<0.05$, #, $P<0.01$ (Kruskal Wallis test). **F, G**, S-nitrosylation of GRK2 in GRK2 immunoprecipitates from hearts of GRK2 Tg and GRFK2/eNOS mice after ischemia-reperfusion, as determined by a Cys-NO antibody. A representative blot for SNO-GRK2 and total GRK2 after immunoprecipitation (**F**). The fold change (compared to sham-operated GRK2 Tg mice) of SNO-GRK2/GRK2 in GRK2 Tg and GRK2/eNOS mice after ischemia-reperfusion (**G**). *, $P<0.05$ (Mann-Whitney test, n=5 mice/group).

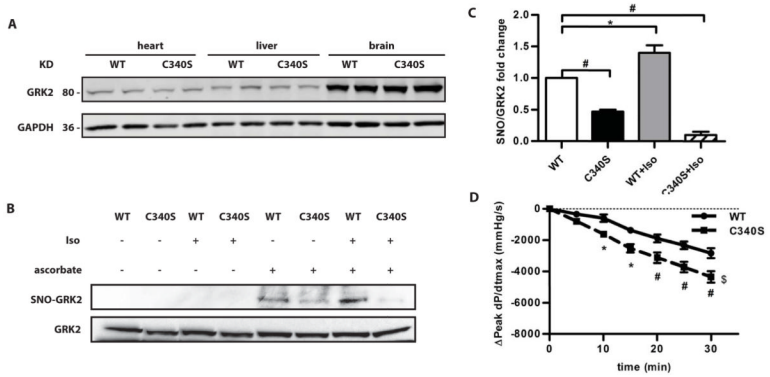

Fig. 3.

Evaluation of the baseline phenotype of GRK2-C340S knock-in mice. **A**, Western blot for GRK2 in the heart, liver and brain from WT mice and GRK2-C340S knock-in mice. GAPDH was used as a loading control. A Western blot representative of 4 independent experiments is shown. **B**, SNO-GRK2 in WT and GRK2-C340S knock-in mouse hearts under basal conditions and 15 min after a bolus injection of isoproterenol (ISO). A representative result from SNO-RAC assay with SNO-GRK2 (top panel) and total GRK2 (bottom panel) under the different conditions is shown. **C**, S-nitrosylated GRK2 in the various genotypes normalized to S-nitrosylated GRK2 in WT heart under baseline conditions. *, $P<0.01$, #, $P<0.05$ (Kruskal Wallis test, n=4–6 mice/group). **D**, Decline in the *in vivo* cardiac contractility (indicated by a decline in peak LV dP/dt_{max}) over 30 min during a maintained ISO infusion in WT and GRK2-C340S mice. *, $P<0.05$, #, $P<0.01$, $, $P<0.05$ C340S curve compared to WT (two way ANOVA, n=4–6 mice/group).

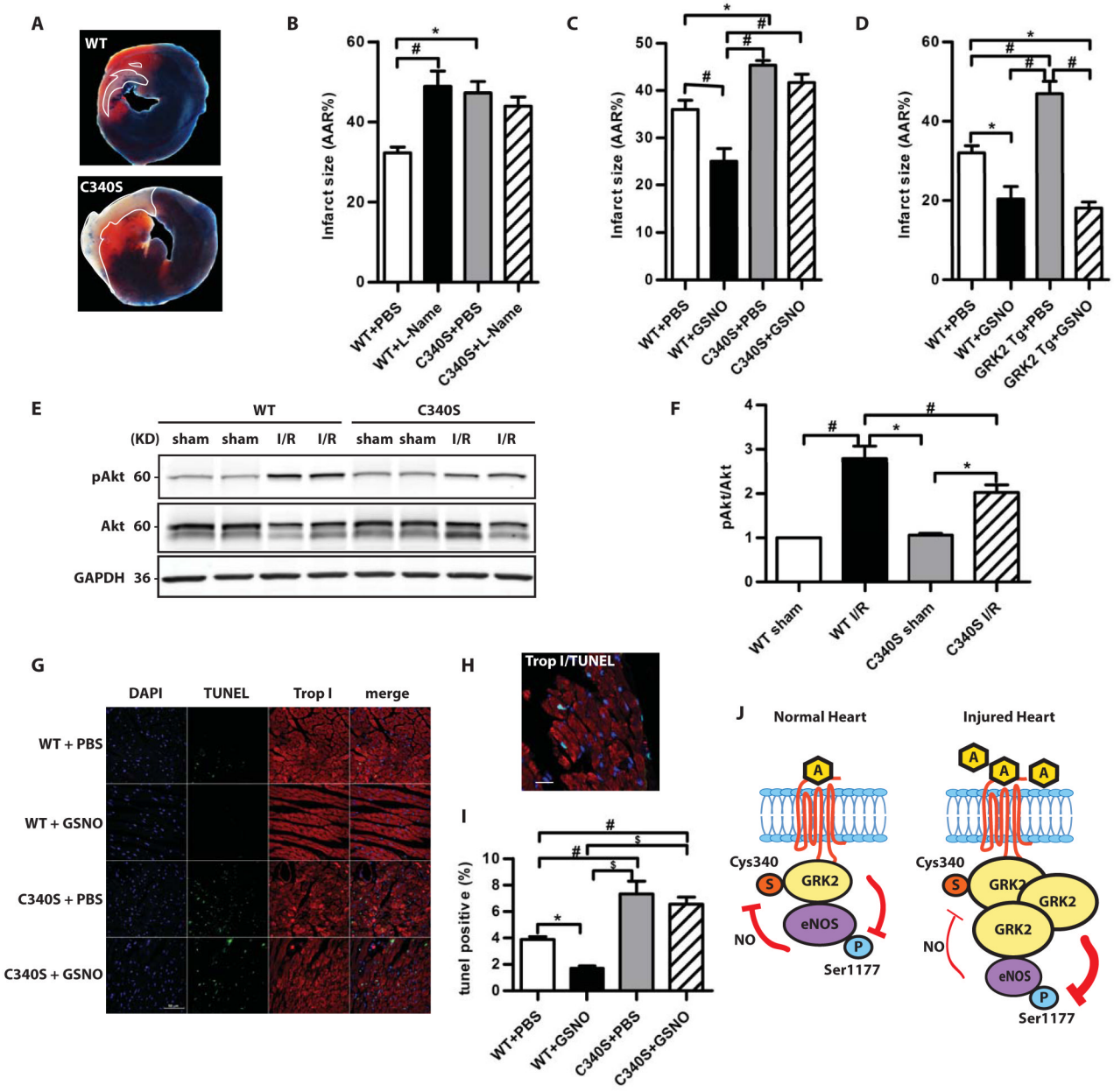

Fig. 4.

The susceptibility of GRK2-C340S knock-in mice to ischemia/reperfusion injury. **A**, Representative images of Evan's Blue/TTC staining of hearts after ischemia/reperfusion. **B**, Quantification of infarct size as a percentage of LV AAR in WT and GRK2-C340S knock-in mice with or without NOS inhibition (L-NAME) (*, $P<0.05$, #, $P<0.01$, ANOVA, n=6–9 mice/group); with or without GSNO infusion (**C**). (*, $P<0.01$, #, $P<0.001$, ANOVA, n=6–7 mice/group); in WT and GRK2 Tg mice with or without GSNO infusion (**D**). (*, $P<0.01$, #, $P<0.001$, ANOVA, n=6 mice/group). **E**, Representative Western blot of pAkt (Ser^{476}), total Akt and GAPDH in sham and post-ischemia/reperfusion WT and GRK2-C340S hearts. **F**, pAkt/Akt ratio normalized to that of the WT sham group as done in (**E**). *, $P<0.05$, #, $P<0.01$ (Kruskal Wallis test, n=7 mice/group). **G**, Representative TUNEL staining (green) of WT and GRK2-C340S heart post-ischemia/reperfusion with or without GSNO infusion.

DAPI staining (blue) marked nuclei and Troponin I staining (red) labeled cardiac myocytes. Scale: 50 μM. **H**, Double labeling of TUNEL and Troponin I staining to show TUNEL positive cardiomyocytes. Scale: 20μM. **I**, The percentage of TUNEL positive nuclei in WT and GRK2-C340S hearts following ischemia/reperfusion injury. *, $P<0.05$, #, $P<0.01$, $, $P<0.001$ (ANOVA, n=6–8 mice/group). **J**, Interdependence of GRK2 and eNOS in the heart.